



Ionization in a laser-assisted ion-ion collisionO. Novak * and R. Kholodov*Institute of Applied Physics, National Academy of Sciences of Ukraine, Petropavlivska Street 58, 40000 Sumy, Ukraine*A. N. Artemyev *Institut für Physik and CINsAT, Universität Kassel, Heinrich-Plett-Straße 40, 34132 Kassel, Germany*A. Surzhykov *Physikalisch-Technische Bundesanstalt, Bundesallee 100, 38116 Braunschweig, Germany
and Institut für Mathematische Physik, Technische Universität Braunschweig, Mendelssohnstraße 3, 38106 Braunschweig, Germany*Th. Stöhlker *Helmholtz Institute Jena, Fröbelstieg 3, 07743 Jena, Germany;
GSI Helmholtzzentrum für Schwerionenforschung, Planckstraße 1, 64291 Darmstadt, Germany;
and Institute for Optics and Quantum Electronics, Friedrich Schiller University, Max-Wien-Platz 1, 07743 Jena, Germany*

(Received 29 March 2023; accepted 19 May 2023; published 31 May 2023)

The ionization of a hydrogenlike heavy ion by the impact of a charged projectile under simultaneous irradiation by a short laser pulse is investigated within the nonperturbative approach, based on numerical solutions of the time-dependent Dirac equation. Emphasis is placed on the question of whether the laser- and impact-ionization channels interfere with each other and how this interference affects the ionization probability. To answer this question we perform detailed calculations for the laser-assisted collisions between hydrogenlike Pb^{81+} and α particles. The results of the calculations clearly indicate that for the experimentally relevant set of (collision and laser) parameters, the interference contribution can reach 10% and can be easily controlled by varying the laser frequency.

DOI: [10.1103/PhysRevA.107.052815](https://doi.org/10.1103/PhysRevA.107.052815)**I. INTRODUCTION**

Recent advances in ion accelerator and coherent light facilities open new possibilities for the exploration of the strong-field domain. Indeed, heavy highly charged ions and intense laser pulses provide a laboratory test bed for investigations of the physics of critical (or even overcritical) electromagnetic fields. For example, laser facilities being constructed in the frame of the Extreme Light Infrastructure project [1] promise to reach electric-field strength comparable with the Schwinger limit [2]. An increase in maximum pulse power is closely related to the shortening of pulse duration, and presently short pulses of only a few optical cycles can be generated [3–5]. Another source of strong yet microscopic electromagnetic fields is highly charged heavy ions. Experiments with heavy ions in a controlled charge state up to bare uranium nuclei are currently performed and planned at the GSI and the Facility for Antiproton and Ion Research (FAIR) facility in Darmstadt [6–10]. The experiments with merging ion beams counterpropagating to a petawatt laser pulse are also anticipated at these facilities. The studies of the interaction of fast moving highly charged ions with laser pulses are also intended at the Gamma Factory in CERN [11].

In the Gamma Factory setup, the laser in the rest frame of ions experiences a Doppler boost of both the field strength and the photon energy to the x-ray range.

The experiments on laser-ion interactions, which are planned at the GSI, FAIR, and Gamma Factory facilities, will provide many novel opportunities for probing both the structure and dynamics of highly charged ions. For the latter, of special interest is the study of laser-assisted fundamental atomic processes. Indeed, while in the nonrelativistic (low-energy and low- Z) regime the ionization, excitation, capture, and charge-transfer processes in laser-assisted atomic collisions have been explored in detail (see Refs. [12–19]), not much is known about relativistic collisions of highly charged heavy ions. The storage-ring experiments on ion-ion (or ion-atom) collisions in the presence of intense laser radiation may therefore provide more insight into the electron dynamics in the strong-field regime.

This paper focuses on the ionization, which is one of the most fundamental processes in atomic physics. The ionization of heavy highly charged ions that is mediated by either relativistic collisions [20–32] or high-intensity laser pulses [33–44] has been studied for many decades. Much less attention has been paid, however, to the ionization in the combined field of a projectile and of a laser. Here we address the question of whether the simultaneous perturbation of an ion by a charged projectile and a strong laser may lead

*Corresponding author: novak-o-p@ukr.net

to remarkable interference effects that modify the ionization probability.

In order to calculate the probability of the laser-assisted ionization in ion collisions and hence to investigate the laser plus collision interference we have developed a nonperturbative approach based on solutions of the time-dependent Dirac equation. This equation describes the interaction of an electron with both a laser pulse and a Coulomb field of a charged projectile. As discussed in Secs. II A and II B, the Coulomb potential of a projectile is taken into account within the monopole approximation, while the coupling to a laser field is treated within the dipole approximation. The numerical solution of the Dirac equation and the evaluation of the ionization probability are reviewed in Sec. II C. The ionization probability, as obtained by using the developed nonperturbative approach, accounts for both Coulomb and laser interactions, as well as for their interference. This interference effect is of nonperturbative nature, as demonstrated in Sec. III, where we consider the case of a weak laser and projectile potentials, which lead to the perturbative limit where the ionization probability is just an incoherent sum of laser-only and collision-only probabilities. Based on this finding, we introduce the relative difference between nonperturbative and perturbative probabilities, which is used to quantify the laser plus Coulomb interference effect. While the developed theory can be used for a wide range of collision systems, in the present work we restrict our analysis to the laser-assisted scattering of α particles off hydrogenlike Pb^{81+} ions. The physical parameters and computational details for this system are given in Sec. IV and the results of the calculations are presented in Sec. V. In particular, we find that the laser plus Coulomb interference may result in significant (about 10%) modification of the ionization probability and, moreover, can be both constructive and destructive depending on the frequency of applied laser pulse. Finally, a short summary of these results is given in Sec. VI.

The relativistic unit system $\hbar = m = c = 1$ is used, unless stated otherwise.

II. THEORETICAL BACKGROUND

In order to analyze the laser-induced ionization of hydrogenlike ions colliding with bare projectile we have to discuss first the building blocks of this process. In Secs. II A and II B we will recall ion-impact-ionization and characterization of the laser pulse, respectively. The theory that accounts for both collision ionization and photoionization will be presented in Sec. II C.

A. Coulomb ionization in ion-ion collisions

Below we will briefly recall the basic theory to describe the ionization of a hydrogenlike ion, colliding with a bare nucleus. We will describe this process in spherical coordinates, whose origin is located at the nucleus of the target (hydrogenlike) ion (see Fig. 1). The projectile is assumed to be light enough to neglect the recoil of the target nucleus during the collision. Moreover, it follows the Rutherford scattering trajectory $\vec{R}(t)$. If the collision energy is sufficiently low, one can also neglect the magnetic field of the moving nucleus.

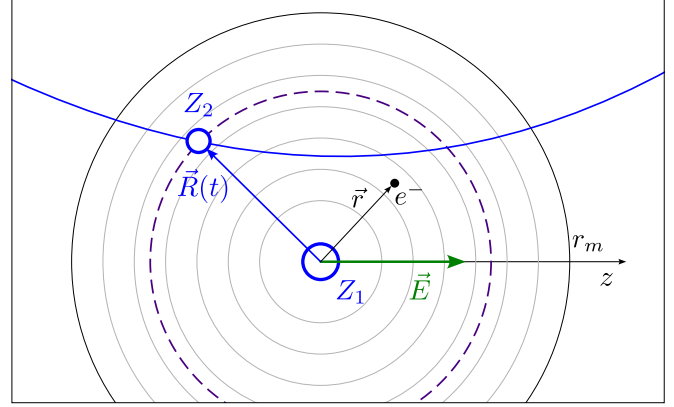


FIG. 1. System layout in the spherical coordinates: \vec{E} is the laser-field vector, the dashed circle represent the charged shell of the monopole part of the projectile potential, and r_m is the boundary for B -spline calculations. The concentric circles illustrate B -spline node boundaries.

In this study we will describe the Coulomb interaction between the target electron and the projectile ion within the monopole approximation. This approximation is known to reproduce the accurate results at small internuclear distances up to approximately 500 fm and is widely used to study the processes involving heavy ions [20–24]. Ionization takes place predominantly at very small internuclear distances, which makes the monopole basis suitable for numerical calculations. Within the monopole approach, the electron-projectile interaction is approximated by the potential of a hollow charged shell of radius $R(t)$ centered at the origin of coordinate system. In this case, the Hamiltonian of an electron in the field of colliding nuclei is given by

$$\hat{H}_0 = \vec{\alpha} \vec{p} + \beta m - \frac{\alpha Z_T}{\max(r, R_T)} - \frac{\alpha Z_P}{\max(r, R(t))}, \quad (1)$$

where α is the fine-structure constant, $\vec{\alpha}$ and β are the Dirac matrices, and R_T is the radius of a target nucleus. Since the monopole Hamiltonian (1) is spherically symmetric, its eigenfunctions can be conveniently written as

$$\Phi_{n\kappa}^\mu(\vec{r}) = \frac{1}{r} \begin{pmatrix} G_{n\kappa}(r) \chi_\kappa^\mu \\ i F_{n\kappa}(r) \chi_{-\kappa}^\mu \end{pmatrix}, \quad (2)$$

where $G_{n\kappa}(r)$ and $F_{n\kappa}(r)$ are the real radial functions and χ_κ^μ denotes a standard Dirac spin-angular function. As usual for the case of spherically symmetric potentials, electronic states are described by the principal quantum number n , the projection μ of the total angular momentum to the z axis, and the spin-orbit quantum number defined as

$$\kappa = (-1)^{j+l+1/2} (j + \frac{1}{2}) \quad (3)$$

so that orbital l and total j angular momenta are given by

$$l = \begin{cases} \kappa, & \kappa > 0 \\ -\kappa - 1, & \kappa < 0 \end{cases}, \quad j = |\kappa| - \frac{1}{2}. \quad (4)$$

The large and small radial components $G_{n\kappa}(r)$ and $F_{n\kappa}(r)$ satisfy the set of differential equations

$$\begin{aligned} \frac{dF_{n\kappa}}{dr} - \frac{\kappa}{r}F_{n\kappa} &= -[\mathcal{E} - V_C(R, r) - 1]G_{n\kappa}, \\ \frac{dG_{n\kappa}}{dr} + \frac{\kappa}{r}G_{n\kappa} &= -[\mathcal{E} - V_C(R, r) + 1]F_{n\kappa}, \end{aligned} \quad (5)$$

where $V_C(R, r)$ is the Coulomb part of the Hamiltonian \mathcal{H}_0 . In order to construct these functions we use the standard dual-kinetically balanced B -spline approach [45,46]. The calculations are performed using 300 B splines of order 8 within a box of a size $r_m \approx 300$ relativistic units. To compute the ionization probability we use a set of about 3500 wave functions Φ_n corresponding to bound and positive quasicontinuum states with $-1.0 < \mathcal{E}_n < 2.5$ and $|\kappa| \leq 8$.

B. Shape of the laser pulse

To account for the laser field, we define its potential in the Coulomb gauge. Below we will consider the vector potential \vec{A} of the form

$$\vec{A}(\eta) = \frac{\vec{e}_z E}{\omega} g(\eta) \cos(\eta + \phi), \quad (6)$$

where $\eta = \omega t - \vec{k}\vec{r}$, ϕ is a phase value, and

$$g(\eta) = \begin{cases} \sin^2\left(\frac{\pi\eta}{\omega T_p}\right) & \text{for } 0 < \eta < \omega T_p \\ 0 & \text{otherwise} \end{cases} \quad (7)$$

is an envelope function that describes a short pulse with a duration T_p of a few optical cycles. The vector potential (6) describes incident light, linearly polarized along the z axis, with the central frequency ω , the amplitude of the electric-field strength E , and pulse duration T_p .

The theoretical analysis of the laser-induced ionization can be significantly simplified if the electron coupling to the laser pulse is treated within the dipole approximation. In this case $\eta \approx \omega t$ and the vector potential (6) is given by

$$\vec{A}(t) = \frac{\vec{e}_z E}{\omega} \sin^2\left(\frac{\pi t}{T_p}\right) \cos(\omega t + \phi). \quad (8)$$

With approximations made for Coulomb and laser potentials, the problem has axial symmetry relative to the z axis. Therefore, the angular momentum projection on this axis is conserved and the quantum number μ does not change during ionization.

C. Solution of the time-dependent problem

Having briefly discussed the shape of the incident laser pulse and the Dirac equation of an electron in the Coulomb field of two nuclei, we are ready to investigate the laser-induced impact ionization. To find the probability of this ionization process, we have to solve the time-dependent Dirac equation of an electron in a combined potential of two nuclei and a laser wave:

$$i \frac{\partial \Psi(\vec{r}, t)}{\partial t} = [\hat{\mathcal{H}}_0 - e\vec{\alpha}\vec{A}(t)]\Psi(\vec{r}, t). \quad (9)$$

The solution of Eq. (9) is constructed in the form of an ansatz

$$\Psi(\vec{r}, t) = \sum_{\mathbf{n}} a_{\mathbf{n}}(t) \Phi_{\mathbf{n}}(\vec{r}, R(t)), \quad (10)$$

where conveniently boldface indices denote sets of quantum numbers $\mathbf{n} = n, \kappa, \mu$. Functions $\Phi_{\mathbf{n}}(\vec{r}, R(t))$ comprise a quastationary basis, defined at each fixed moment of time t as the eigenfunctions of the two-center Hamiltonian $\hat{\mathcal{H}}_0$ for the corresponding value of the distance R ,

$$\hat{\mathcal{H}}_0 \Phi_{\mathbf{n}}(\vec{r}, R) = \mathcal{E}_{\mathbf{n}} \Phi_{\mathbf{n}}(\vec{r}, R). \quad (11)$$

Let us note that application of wave functions (11) allows us to include the interaction of the escaping electron with the combined Coulomb potential of both nuclei to all orders, so additional Coulomb corrections to the ionization probability are not needed. For the sake of brevity, below we will omit the arguments of the basis wave functions $\Phi_{\mathbf{n}}$.

By substituting the expansion (10) into the Dirac equation (9), we obtain the system of coupled differential equations to determine the amplitudes $a_{\mathbf{n}}(t)$:

$$i\dot{a}_{\mathbf{n}}(t) = M_{\mathbf{n}\mathbf{k}} a_{\mathbf{k}}(t), \quad (12)$$

$$M_{\mathbf{n}\mathbf{k}} = \mathcal{E}_{\mathbf{k}} \delta_{\mathbf{n}\mathbf{k}} - i\langle \Phi_{\mathbf{n}} | \dot{\Phi}_{\mathbf{k}} \rangle - eA(t) \langle \Phi_{\mathbf{n}} | \alpha_3 | \Phi_{\mathbf{k}} \rangle. \quad (13)$$

Taking the derivative with respect to time of the equations

$$\langle \Phi_{\mathbf{n}} | \mathcal{H}_0 | \Phi_{\mathbf{k}} \rangle = \mathcal{E}_{\mathbf{n}} \delta_{\mathbf{n}\mathbf{k}}, \quad \langle \Phi_{\mathbf{n}} | \Phi_{\mathbf{k}} \rangle = \delta_{\mathbf{n}\mathbf{k}}, \quad (14)$$

we can rewrite the matrix element $\langle \Phi_{\mathbf{n}} | \dot{\Phi}_{\mathbf{k}} \rangle$ as [2]

$$\langle \Phi_{\mathbf{n}} | \dot{\Phi}_{\mathbf{k}} \rangle = \frac{\langle \Phi_{\mathbf{n}} | \dot{\mathcal{H}}_0 | \Phi_{\mathbf{k}} \rangle}{\mathcal{E}_{\mathbf{k}} - \mathcal{E}_{\mathbf{n}}}. \quad (15)$$

Thus, the matrix elements $M_{\mathbf{n}\mathbf{k}}$ are

$$M_{\mathbf{n}\mathbf{k}} = \mathcal{E}_{\mathbf{k}} \delta_{\mathbf{n}\mathbf{k}} - i \frac{\langle \Phi_{\mathbf{n}} | \dot{\mathcal{H}}_0 | \Phi_{\mathbf{k}} \rangle}{\mathcal{E}_{\mathbf{k}} - \mathcal{E}_{\mathbf{n}}} - eA(t) \langle \Phi_{\mathbf{n}} | \alpha_3 | \Phi_{\mathbf{k}} \rangle. \quad (16)$$

To further simplify the system of equations (12)–(16), we note that the time derivative acts on the Hamiltonian \mathcal{H}_0 only via its dependence on the internuclear distance $R(t)$. Hence, we can write this derivative as a sum of its radial and angular parts

$$\frac{\partial}{\partial t} = \dot{R} \frac{\partial}{\partial R} - i(\vec{\Omega} \hat{j}), \quad (17)$$

where $\vec{\Omega}$ is the angular velocity of the internuclear axis and \hat{j} is the electron angular momentum operator. The matrix elements of the second term in Eq. (17) are known to vanish at small internuclear distances [21]. The first matrix element on the right-hand side of Eq. (16) can be written as

$$\frac{\langle \Phi_{\mathbf{n}} | \dot{\mathcal{H}}_0 | \Phi_{\mathbf{k}} \rangle}{\mathcal{E}_{\mathbf{k}} - \mathcal{E}_{\mathbf{n}}} = \frac{\dot{R}}{\mathcal{E}_{\mathbf{k}} - \mathcal{E}_{\mathbf{n}}} \langle \Phi_{\mathbf{n}} | \frac{dV_C(R)}{dR} | \Phi_{\mathbf{k}} \rangle. \quad (18)$$

Solution of the system of coupled equations (12) requires evaluation of matrix elements of the operator $dV_C(R)/dR$ for different internuclear distances R . Having performed these calculations and computing the matrix element of the operator α_3 , we are ready to find amplitudes $a_{\mathbf{n}}(t)$ numerically.

For the numerical solution of the system of equations (12) we split the time into small intervals Δt . For each time interval the matrix M is approximated by its middle value $M(t) \approx M(t_i + \Delta t/2)$, $t \in [t_i, t_{i+1}]$. When M is approximated by a

constant matrix, the solution of the set of equations (12) can be found as

$$\vec{a}_j(t_i + \Delta t) = e^{-iM\Delta t} \vec{a}_j(t_i). \quad (19)$$

However, computation of the matrix exponent may be very demanding. Instead, we use the highly efficient Lanczos propagation method to find the vector $\vec{a}(t)$ [47]. After performing the time propagation of the amplitudes a_n to $t = \infty$, we can find for the ionization probability

$$w_{\alpha\gamma} = \sum_{\mathbf{n}} |a_{\mathbf{n}}(t = \infty)|^2, \quad (20)$$

where the summation runs over all electronic states, belonging to the positive-energy quasicontinuum, i.e., when $\mathcal{E}_{\mathbf{n}} > 1$.

III. PERTURBATIVE CASE

Before discussing the results of the nonperturbative treatment of the laser-induced collisional ionization, it is useful to briefly consider the predictions of the perturbation theory. In the case of weak laser and projectile potentials, the amplitudes near the matrix elements in Eq. (16) can be approximated as $a_{\mathbf{k}} \approx 1$ for the initial state and $a_{\mathbf{k}} \rightarrow 0$ otherwise. Then the set of ordinary differential equations (12) can be decoupled [2,21], and we obtain the ordinary differential equation

$$i\dot{a}_{\mathbf{n}} = \mathcal{E}_{\mathbf{n}} a_{\mathbf{n}} - i\hat{R} \frac{\langle \Phi_{\mathbf{n}} | \frac{dV_C}{dR} | \Phi_{\mathbf{k}} \rangle}{\mathcal{E}_{\mathbf{n}} - \mathcal{E}_{\mathbf{k}}} - eA(t) \langle \Phi_{\mathbf{n}} | \alpha_3 | \Phi_{\mathbf{k}} \rangle \quad (21)$$

for the probability amplitude of the transition from the initial state \mathbf{k} to the final state \mathbf{n} . In order to analyze the symmetry properties of Eq. (21) we recall that eigensolutions (2) of the spherically symmetric (monopole) Hamiltonian \mathcal{H}_0 are characterized by the Dirac angular momentum quantum number \varkappa . We consider ionization from the $1s$ ground state for which $\varkappa = -1$. A simple angular algebra analysis shows that the matrix element of the operator dV_C/dR has nonzero values only for transitions without a change of \varkappa . At the same time, the matrix element of α_3 allows transitions to the states with $\varkappa = -2$ and 1 . Based on these observations as well as on Eq. (20), we see that the total ionization probability is given by the sum of collision-only and laser-only probabilities, with no interference between these two channels. As we will see below, this is not the case for the nonperturbative treatment, where the interference between Coulomb- and laser-ionization terms may remarkably modify the ionization probability. In order to investigate this interference effect, we introduce the relative difference

$$\delta w_{\alpha\gamma} = \frac{w_{\alpha\gamma} - (w_{\alpha} + w_{\gamma})}{w_{\alpha} + w_{\gamma}} \quad (22)$$

between the probability $w_{\alpha\gamma}$ of the ionization by a combined Coulomb plus laser potential and the sum of Coulomb-only w_{α} and laser-only w_{γ} probabilities. The two latter are obtained based on Eq. (16) with the third and second terms omitted, respectively.

IV. DETAILS OF CALCULATIONS

While the developed approach can be applied for various ion collisions, here we consider ionization of a hydrogenlike

Pb^{81+} ion by a combined potential of a projectile α particle and a short intense laser pulse. We will investigate the ionization probability (20) of this process, which depends on a number of physical parameters which are discussed below. First, according to Eq. (8), the laser pulse is defined by its duration T_p , frequency ω , maximum field strength E , and carrier-envelope phase ϕ . To quantify field strength and frequency, we introduce characteristic values

$$\omega' = 2\mathcal{E}_{\text{bind}}, \quad (23a)$$

$$E' = \frac{3\alpha Z_T}{\langle r^2 \rangle}, \quad (23b)$$

where $\mathcal{E}_{\text{bind}}$ is the binding energy and $\langle r^2 \rangle$ is the mean square of the radial electron coordinate in the ground state of the target Pb^{81+} ion. We note that Eqs. (23) are similar to the nonrelativistic Z scaling of the frequency and the electric-field strength [38,41]. This scaling, however, is still practical to quantify the strength E and to define weak- and strong-field regimes.

In the present work we perform calculations of the ionization probability for the laser frequency and field strength in the ranges of $0.4\omega' \leq \omega \leq 2.0\omega'$ and $10^{-3}E' \leq E \leq 1.0E'$. For these parameters, the electron-laser coupling can be treated within the dipole approximation. To justify the dipole approach we follow Ref. [33] and recall that an electron in a field of an electromagnetic wave oscillates along the figure-eight-shaped trajectory. The corresponding displacement, or the amplitude of electron oscillations, can be written as

$$X = \frac{1}{2\omega} \frac{U_p}{m + 2U_p}, \quad (24)$$

where U_p is the ponderomotive potential

$$U_p = \frac{e^2 E^2}{4m\omega^2}. \quad (25)$$

In order to apply the dipole approximation, the amplitude X should be small compared to the laser wavelength λ as well as to the size of the electron orbit r_B . For the laser frequencies studied in the present work, the corresponding relations are

$$\begin{aligned} 2.5 \times 10^{-9} &\leq X/\lambda \leq 6.3 \times 10^{-8}, \\ 1.3 \times 10^{-8} &\leq X/r_B \leq 1.6 \times 10^{-6} \end{aligned} \quad (26)$$

for the weak field $E = 0.001E'$ and

$$\begin{aligned} 2.4 \times 10^{-3} &\leq X/\lambda \leq 2.4 \times 10^{-2}, \\ 1.2 \times 10^{-2} &\leq X/r_B \leq 0.64 \end{aligned} \quad (27)$$

for the stronger-field regime $E = E'$. We may conclude, therefore, that the dipole approximation is applicable for our studies, at least when the laser field is not too strong. This conclusion is further supported by the comparison between dipole and higher multipole calculations reported in Ref. [41].

Besides the frequency ω , the field strength E , and the envelope parameters, one should also agree at which moment of the collision the laser pulse comes. To specify this time we introduce a time interval between the moment of the closest nucleus approach $t(R_{\text{min}})$ and the moment of the maximum pulse intensity $t(I_{\text{max}})$,

$$\tau = t(R_{\text{min}}) - t(I_{\text{max}}). \quad (28)$$

In Sec. V we will investigate how the ionization probability depends on τ . The calculations performed for a well-defined time interval [see Eq. (28)] are however of theoretical academic interest. To investigate a more realistic scenario, we average the ionization probability over some measurement window with respect to the interval τ . Apparently, the size of the window cannot be unambiguously defined within the theoretical framework. In the present work we define it as

$$-2T_p \leq \tau \leq 2T_p, \quad (29)$$

where T_p is the pulse duration. In the calculations below we set $T_p = 3T$, where T is the period of the optical cycle. Moreover, we assume that the carrier-envelope phase is zero $\phi = 0$.

Apart from the laser parameters, discussed above, one also needs to define the impact parameter ρ and the energy $\mathcal{E}_{c.m.}$ that characterize the ion-ion collision. We perform calculations for collisions with center-of-mass energies $\mathcal{E}_{c.m.} = 5$ and 10 MeV and impact parameters up to 500 fm.

In theory, the electron wave function should be propagated from $t = -\infty$ to $t = +\infty$, with a single lead ion in the initial and final states. In practice, however, one needs to set the maximum distance between nuclei large enough to ensure the numerical convergence of the results. It was found that the best results can be obtained with the initial and final internuclear separations set to be equal. For this choice of parameters the results are numerically stable for the maximum distance between nuclei set to 10^5 fm.

To conclude the discussion of the numerical procedure, we describe the technique used which allows significant reduction in the computational resources. Note that on the right-hand side of Eq. (18) only $\dot{R}(t)$ depends on the collision parameters $\mathcal{E}_{c.m.}$ and ρ , while the matrix element depends only on the value of R and the type of nuclei. Similarly, the matrix $\langle \Phi_n | \alpha_3 | \Phi_k \rangle$ in Eq. (16) does not depend on the laser pulse potential. This allows us to reuse the calculated matrices for collisions with different collision energies and laser pulse parameters.

V. RESULTS AND DISCUSSION

Before we start our analysis of the ground-state ionization for Pb^{81+} by the combined laser plus Coulomb potential, let us briefly discuss the individual collision-only w_α , and laser-only w_γ probabilities. Figure 2 shows, for example, the probability of the $1s$ ionization by α -particle impact. The calculations were performed for two scenarios: In Fig. 2(a) we display w_α as a function of impact parameter ρ but for the fixed center-of-mass energy $\mathcal{E}_{c.m.} = 10$ MeV, while Fig. 2(b) presents the energy dependence of w_α for the case $\rho = 0$. The impact parameter dependence features a local maximum at approximately 50 fm and decreases polynomially for the higher impact parameters.

We note that the ρ behavior of w_α , as well as the monotonic increase of the ionization probability with the center-of-mass energy, displayed in Fig. 2, is expected from previous studies [25–28].

In order to investigate the ionization of the $1s$ electron for hydrogenlike lead by a laser pulse, we display in Fig. 3 the ionization probability w_γ as a function of (relative) frequency ω [Fig. 3(a)] and field strength [Fig. 3(b)]. The calculations

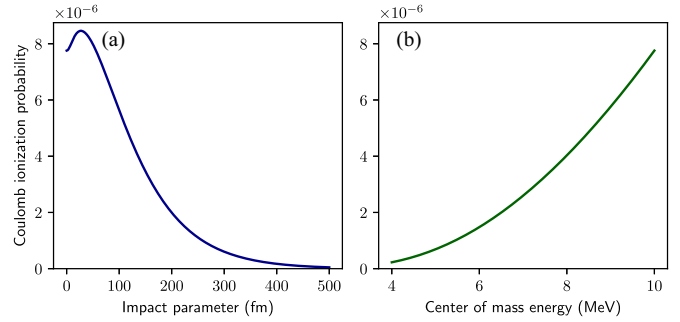


FIG. 2. Probability w_α of the ground-state ionization of hydrogenlike lead by an α particle impact: (a) w_α , calculated for the center-of-mass energy $\mathcal{E}_{c.m.} = 10$ MeV, as a function of impact parameter ρ and (b) energy dependence of the ionization probability for the head-on collision, $\rho = 0$.

of $w_\gamma(\omega)$ are performed for two field strengths: $E = 10^{-3}E'$ (blue dash-dotted line) and $E = 1.0E'$ (green solid line). For the weak field, w_γ has a maximum near the value of $\omega \approx \mathcal{E}_{\text{bind}}$ and for both strengths w_γ has an exponential tail at higher frequencies. In Fig. 3(b) we display $w_\gamma(E)$ as a function of electric-field strength and calculated for two laser frequencies $\omega = 0.5\omega'$ (green solid line) and $\omega = 2.0\omega'$ (blue dash-dotted line). The photoionization probability scales as the square of the laser-field strength for small E [41–44].

Having briefly discussed the ionization probabilities for the laser-only and collision-only cases, we are ready to explore the ionization by the combined laser plus Coulomb potential. The probability $w_{\alpha\gamma}$ is presented as a function of impact parameter ρ in Figs. 4 and 5 and a function of relative laser frequency ω/ω' in Figs. 6 and 7. The probability presented in these figures is averaged over the measurement window (29) with respect to the time offset τ , as explained before. In order to investigate the effect of the interference between laser and Coulomb ionization channels, we display also the sum of individual (laser-only and collision-only) probabilities. Moreover, the relative difference, as defined in Eq. (22), is displayed in Figs. 4(b), 5(b), 6(b), and 7(b).

First, we discuss the ρ dependence of the ionization probability, which is calculated for the center-of-mass energy $\mathcal{E}_{c.m.} = 10$ MeV, both laser-field strengths $E = 10^{-3}E'$

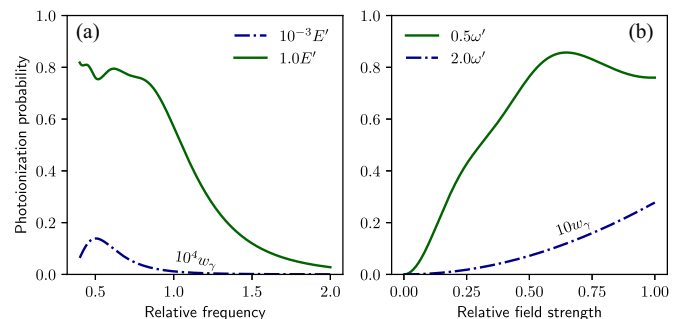


FIG. 3. Probability of photoionization of a hydrogenlike Pb by a laser pulse as a function of (a) relative laser frequency ω/ω' and (b) relative field strength E/E' . The blue dash-dotted curve is scaled by a factor (a) 10^4 and (b) 10^1 .

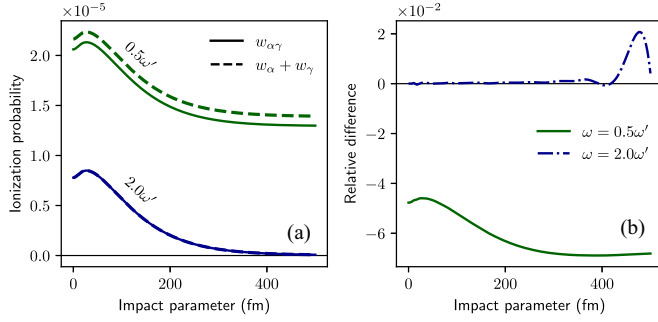


FIG. 4. (a) Probability $w_{\alpha\gamma}$ of the $1s$ ionization of hydrogenlike Pb^{81+} by a combined potential of the laser pulse and α particle as a function of impact parameter. Calculations were performed for the center-of-mass energy $\mathcal{E}_{\text{c.m.}} = 10$ MeV, laser-field strength $E = 10^{-3}E'$, and laser frequencies $\omega = 0.5\omega'$ (green solid line) and $\omega = 2.0\omega'$ (blue solid line). Moreover, we compare $w_{\alpha\gamma}$ with the incoherent sum of laser-only and collision-only probabilities (green and blue dashed lines). (b) Relative difference $\delta w_{\alpha\gamma}$ between the probability of ionization by a combined potential and the sum of ionization probabilities by separate potentials.

(Fig. 4) and $E = E'$ (Fig. 5), and two laser frequencies $\omega = 0.5\omega'$ (green line) and $\omega = 2.0\omega'$ (blue line). As seen from the figures, the interference between the laser and Coulomb channels may lead to a remarkable modification of the ionization probability $w_{\alpha\gamma}$ with respect to the incoherent sum $w_{\alpha} + w_{\gamma}$. For example, $\delta w_{\alpha\gamma}$ can reach approximately 6% for the low laser frequency and low field strength.

Figures 6 and 7 allow us to discuss the laser frequency dependence of the ionization probability $w_{\alpha\gamma}$. Here we perform calculations for the head-on collisions $\rho = 0$, for two center-of-mass energies $\mathcal{E}_{\text{c.m.}} = 5$ and 10 MeV, and for two laser-field strengths $E = 10^{-3}E'$ (Fig. 6) and $E = E'$ (Fig. 7). Similar to before, we compare $w_{\alpha\gamma}$ with the sum of individual probabilities $w_{\alpha} + w_{\gamma}$ and present in Figs. 6(b) and 7(b) the relative difference (22). As seen from the figures, the Coulomb plus laser interference may again lead to a remarkable modification of the ionization probability. For low laser-field strength (Fig. 6) and low frequency ω , for example, the interference results in approximately 15% reduction of $w_{\alpha\gamma}$ when compared with $w_{\alpha} + w_{\gamma}$. In contrast, for high laser-field strength $E = E'$ (Fig. 7) and frequency $\omega \gtrsim \omega'$ the interference leads to 3–5% enhancement of the ionization probability.

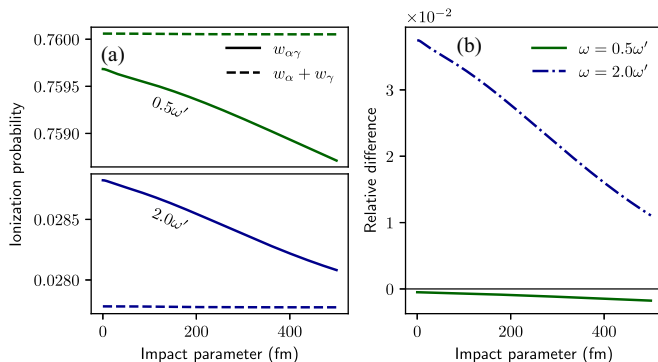


FIG. 5. Same as in Fig. 4 but for the laser-field strength $E = E'$.

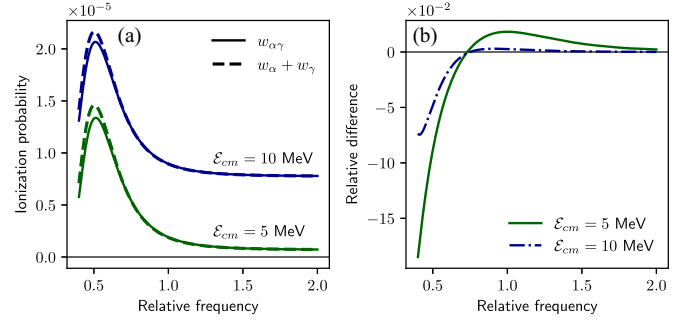


FIG. 6. (a) Probability $w_{\alpha\gamma}$ of the $1s$ ionization of hydrogenlike Pb^{81+} by a combined potential of a laser pulse and an α particle as a function of relative laser frequency ω/ω' . Calculations have been performed for the field strength $E = 10^{-3}E'$ and the impact parameter $\rho = 0$. Moreover, we compare $w_{\alpha\gamma}$ with the incoherent sum of individual laser-only and collision-only probabilities (dashed lines). (b) Corresponding relative difference (22).

It could be concluded from the obtained results that the interference effect has different signs for low and high frequencies. In the case of strong field, the process is dominated by photoionization, with $w_{\gamma} \gg w_{\alpha}$. Nevertheless, the interaction with the projectile nucleus results in the difference between $w_{\alpha\gamma}$ and the incoherent sum $w_{\alpha} + w_{\gamma}$, which is greater than w_{γ} itself.

To better understand the laser plus Coulomb interference, we will consider below the partial probabilities

$$w(\chi_f) = \sum_{n: \mathcal{E}_n > 1} |a_{n\chi_f}^{\mu}|^2 \quad (30)$$

for the ionization of an electron into the continuum state with a particular angular momentum quantum number χ_f . Figure 8 shows the probability of the transition of the initially bound $1s$ electron to continuum states with different χ_f 's. Calculations are done for the particular case of $\tau = 0$, i.e., when the laser pulse intensity reaches its maximum in the moment of the closest nucleus approach. As seen from the figure, the calculations are done for low [Figs. 8(a) and 8(c)] and high laser-field strength [Figs. 8(b) and 8(d)] regimes, as well as for two laser frequencies $\omega = 2.0\omega'$ [Figs. 8(a) and 8(b)] and $\omega = 0.5\omega'$ [Figs. 8(c) and 8(d)]. For all these cases we present the partial ionization probabilities as calculated for the combined laser plus Coulomb potential (right light green bar for each χ_f) and for the incoherent sum of laser-only and collision-only

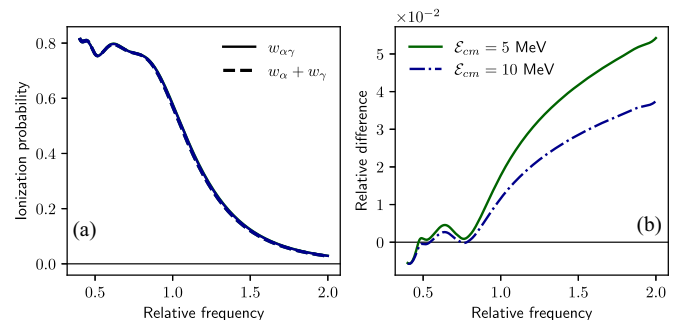


FIG. 7. Same as in Fig. 6 for the laser-field strength $E = E'$.

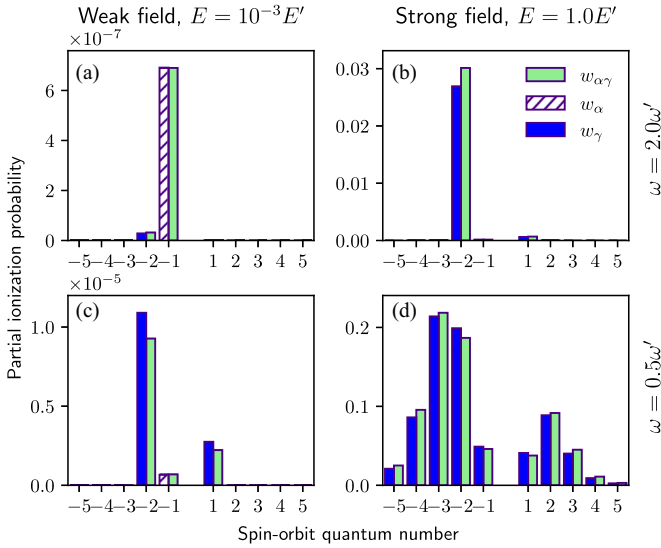


FIG. 8. Partial probability for the ionization of the $1s$ electron to the continuum with particular spin-orbit quantum number κ_f . The calculations were performed for the center-of-mass collision energy $\mathcal{E}_{c.m.} = 5$ MeV, laser-field strengths (a) and (c) $E = 10^{-3}E'$ and (b) and (d) $E = 1.0E'$, and laser frequencies (a) and (b) $\omega = 2.0\omega'$ and (c) and (d) $\omega = 0.5\omega'$. The predictions for the ionization probability $w_{\alpha\gamma}(\kappa_f)$ for the combined laser plus Coulomb potential (green bar) are compared with those for the incoherent sum of individual channels $w_{\alpha}(\kappa_f) + w_{\gamma}(\kappa_f)$.

channels (left bar, with blue color and hatching corresponding to contributions of laser-only and collision-only summands, respectively). As expected, in the case of weak field and for the ionization from the ground $1s$ state, the main channels are $\kappa_f = -2, -1, 1$, in full compliance with the predictions of the perturbation theory from Sec. III. In contrast, for the strong-field regime $E = 1.0E'$, the population of other continuum states increases, especially for low laser frequency.

Figure 8 also clearly illustrates the effect of the interference between the photoionization and impact ionization channels. As seen from the figure, $w_{\alpha\gamma}(\kappa_f)$ remarkably differs from the sum $w_{\alpha}(\kappa_f) + w_{\gamma}(\kappa_f)$ for most of the continuum states κ_f . For example, for the weak-field and low-frequency regime [Fig. 8(c)], the Coulomb-laser interference significantly reduces the partial probabilities for $\kappa_f = -2$ and 1 channels. In turn, this leads to the reduction of the total (summed over κ_f) probability $w_{\alpha\gamma}$ that was observed in Fig. 6.

Until now, we have investigated the Coulomb plus laser contribution to the ionization probability either for the averaged time offset τ between the moments of maximal laser pulse intensity and the closest nucleus approach or for the case $\tau = 0$. To better understand how this interference contribution varies with time, in Figs. 9 and 10 we display the relative difference $\delta w_{\alpha\gamma}(\tau, \kappa_f)$ as a function of τ and for particular continuum-electron channels $\kappa_f = -2, -1, 1$. The calculations have been carried out for two laser frequencies $\omega = 0.5\omega'$ (Fig. 9) and $\omega = 2.0\omega'$ (Fig. 10) as well as for the laser-field strengths $E = 0.001E'$ and $1.0E'$.

As seen from Figs. 9 and 10, the relative difference $\delta w_{\alpha\gamma}(\tau, \kappa_f)$, and hence the Coulomb plus laser interference contribution, is maximal around $\tau = 0$ and tends to zero

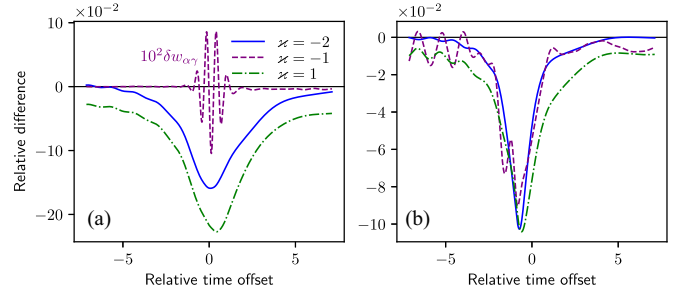


FIG. 9. Relative difference $\delta w_{\alpha\gamma}(\tau, \kappa_f)$ for the ionization into a particular continuum state κ_f as a function of the time offset τ between the moments of closest nucleus approach and the laser pulse maximum. The time offset is shown in units of the optical period. The calculations were performed for the collision center-of-mass energy $\mathcal{E} = 10$ MeV, frequency $\omega = 0.5\omega'$, and laser pulse with the strengths (a) $E = 0.001E'$ and (b) $E = 1.0E'$. In (a) the curve for $\kappa_f = -1$ is scaled by a factor 10^2 .

for large offset times. While this qualitative behavior can be observed for all continuum channels $\kappa_f = -2, -1, 1$, the quantitative values of $\delta w_{\alpha\gamma}(\tau, \kappa_f)$ strongly depend on κ_f . For example, the relative difference for the continuum states with $\kappa_f = -2, 1$, which correspond to the photoionization channels in the perturbative limit, can reach about 10% and the interference can be either destructive (lower frequency, Fig. 9) or constructive (higher frequency, Fig. 10). This behavior can be observed for both weak- and strong-field regimes. In contrast, in the case of the collision channel with $\kappa_f = -1$ and a weak laser field, the relative difference exhibits oscillatory behavior and by orders of magnitude smaller than $\delta w_{\alpha\gamma}$ in the photoionization channels. In the case of larger laser strength the relative difference $\delta w_{\alpha\gamma}(\tau, \kappa_f = -1)$ retains its behavior but increases its magnitude, as can be seen in Fig. 10(b).

By analyzing the time dependence of the relative difference one can notice small oscillations of $\delta w_{\alpha\gamma}(\tau, \kappa_f)$ for collision channels $\kappa_f = -2, 1$ and for $\tau < 0$ [see, for example, Fig. 10(a)]. To explain this behavior, we recall that negative time offsets τ imply that the collision with the projectile happens before the arrival of the laser pulse. In our opinion, the oscillations of $\delta w_{\alpha\gamma}$ can be connected to oscillatory behavior of the time dependence of ionization probability in ion collisions [31]. Indeed, in the case shown in Fig. 10(a), the pulse duration is much less than the typical collision time. Therefore, the system can be considered similarly to the pump-probe setup involving two laser pulses [48,49].

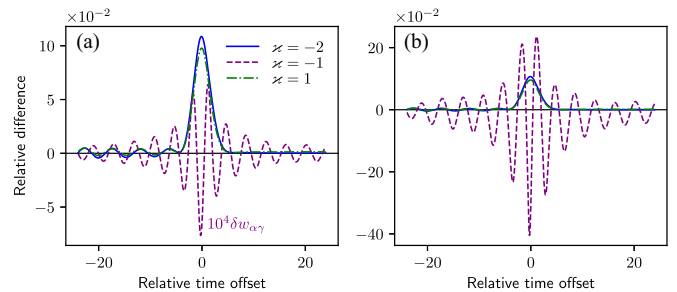


FIG. 10. Same as in Fig. 9 but for laser frequency $\omega = 2.0\omega'$. In (a) the curve for $\kappa_f = -1$ is scaled by a factor 10^4 .

VI. CONCLUSION

We have presented a theoretical study of electron ionization in laser-assisted ion-ion collisions. To calculate the ionization probability, a numerical nonperturbative approach for solution of time-dependent Dirac equation was developed, which accounts for the interaction of the target electron both with a laser pulse and with a Coulomb field of a projectile ion. While our nonperturbative approach can be applied to a variety of collision systems, here we considered a particular case of the laser-assisted scattering of an α particle by hydrogenlike lead being initially in its ground electronic state. Particular attention was paid to the question of how the ionization probability can be affected by the interference between laser and Coulomb interactions. In order to quantify this interference effect we introduced the relative difference between the probability of ionization by a combined (laser plus Coulomb) potential and the sum of probabilities of laser-only and collision-only processes.

The calculations of the relative difference were performed for a set of collision and laser parameters relevant for current experiments. Based on these calculations, we found that the laser plus Coulomb interference may result in up to 10% modification of the ionization probability and the effect becomes more pronounced for low collision energies $\mathcal{E}_{c.m.}$. Moreover, depending on the laser frequency ω , the interference can be either constructive (high ω) or destructive (low ω). These effects can be observed, for example, at the GSI and FAIR facilities in Darmstadt and can provide further insight into laser-induced ion collisions.

ACKNOWLEDGMENTS

This work is partially supported by the grant of the National Academy of Sciences of Ukraine (No. 0121U111794) under the Targeted research program Collaboration in advanced international projects on high-energy physics and nuclear physics.

-
- [1] O. Tesileanu, D. Ursescu, R. Dabu, and N. V. Zamfir, *J. Phys.: Conf. Ser.* **420**, 012157 (2013).
 - [2] W. Greiner, B. Müller, and J. Rafelski, *Quantum Electrodynamics of Strong Fields* (Springer, Berlin, 1985).
 - [3] T. Brabec and F. Krausz, *Rev. Mod. Phys.* **72**, 545 (2000).
 - [4] A. Baltuška, T. Udem, M. Uiberacker, M. Hentschel, E. Goulielmakis, C. Gohle, R. Holzwarth, V. S. Yakovlev, A. Scrinzi, T. W. Hänsch, and F. Krausz, *Nature (London)* **421**, 611 (2003).
 - [5] R. López-Martens, K. Varjú, P. Johnsson, J. Mauritsson, Y. Mairesse, P. Salières, M. B. Gaarde, K. J. Schafer, A. Persson, S. Svanberg, C. G. Wahlström, and A. L'Huillier, *Phys. Rev. Lett.* **94**, 033001 (2005).
 - [6] H. H. Gutbrod, K. D. Groß, W. F. Henning, and V. Metag, An international accelerator facility for beams of ions and anti-protons. Conceptual design report, 2001, <https://inspirehep.net/literature/567994>.
 - [7] A. Gumberidze, F. Bosch, A. Bräuning-Demian, S. Hagmann, T. Kühl, D. Liesen, R. Schuch, T. Stöhlker, for the SPARC Collaboration, *Nucl. Instrum. Methods Phys. Res. Sect. B* **233**, 28 (2005).
 - [8] T. Stöhlker, T. Beier, H. F. Beyer, F. Bosch, A. Bräuning-Demian, A. Gumberidze, S. Hagmann, C. Kozhuharov, T. Kühl, D. Liesen, R. Mann, P. H. Mokler, W. Quint, R. Schuch, and A. Warczak, *Nucl. Instrum. Methods Phys. Res. Sect. B* **235**, 494 (2005).
 - [9] A. Gumberidze, T. Stöhlker, H. F. Beyer, F. Bosch, A. Bräuning-Demian, S. Hagmann, C. Kozhuharov, T. Kühl, R. Mann, P. Indelicato, W. Quint, R. Schuch, and A. Warczak, *Nucl. Instrum. Methods Phys. Res. Sect. B* **267**, 248 (2009).
 - [10] T. Kuehl, V. Bagnoud, T. Stöhlker, Y. Litvinov, D. F. A. Winters, B. Zielbauer, H. Backe, C. Spielmann, J. Seres, A. Tünnemann, P. Neumayer, B. Aurand, S. Namba, and H. Y. Zhao, *J. Phys.: Conf. Ser.* **488**, 142003 (2014).
 - [11] D. Budker, J. R. C. López-Urrutia, A. Derevianko, V. V. Flambaum, M. W. Krasny, A. Petrenko, S. Pustelny, A. Surzhykov, V. A. Yerokhin, and M. Zolotarev, *Ann. Phys. (Berlin)* **532**, 2000204 (2020).
 - [12] L. B. Madsen, J. P. Hansen, and L. Kocbach, *Phys. Rev. Lett.* **89**, 093202 (2002).
 - [13] J. P. Hansen, T. Sørøvik, and L. B. Madsen, *Phys. Rev. A* **68**, 031401(R) (2003).
 - [14] A. B. Voitkiv, N. Toshima, and J. Ullrich, *J. Phys. B* **39**, 3791 (2006).
 - [15] M. F. Ciappina and L. B. Madsen, *J. Phys. B* **39**, 5037 (2006).
 - [16] M. F. Ciappina and L. B. Madsen, *Phys. Rev. A* **77**, 023412 (2008).
 - [17] T. Kirchner, *Phys. Rev. A* **75**, 025401 (2007).
 - [18] F. J. Domínguez-Gutiérrez and R. Cabrera-Trujillo, *Eur. Phys. J. D* **68**, 226 (2014).
 - [19] F. J. Domínguez-Gutiérrez and R. Cabrera-Trujillo, *J. Phys. B* **48**, 135202 (2015).
 - [20] U. Wille and R. Hippler, *Phys. Rep.* **132**, 129 (1986).
 - [21] U. Müller-Nehler and G. Soff, *Phys. Rep.* **246**, 101 (1994).
 - [22] B. Müller, G. Soff, W. Greiner, and V. Ceausescu, *Z. Phys. A* **285**, 27 (1978).
 - [23] A. Graue, J. Hansteen, R. Gundersen, and L. Kocbach, *J. Phys. B* **15**, L445 (1982).
 - [24] K. Rumrich, W. Greiner, G. Soff, K. Wietschorke, and P. Schlüter, *J. Phys. B* **22**, 165 (1989).
 - [25] R. Vader, A. van der Woude, and R. Meijer, *Phys. Rev. A* **14**, 62 (1976).
 - [26] J. Hansteen, *Adv. At. Mol. Phys.* **11**, 299 (1976).
 - [27] J. Hansteen, *Phys. Scr.* **31**, 63 (1985).
 - [28] J. Hansteen, *Phys. Scr.* **42**, 299 (1990).
 - [29] W. E. Meyerhof and K. Taulbjerg, *Annu. Rev. Nucl. Sci.* **27**, 279 (1977).
 - [30] G. Soff, W. Greiner, W. Betz, and B. Müller, *Phys. Rev. A* **20**, 169 (1979).
 - [31] S. R. McConnell, A. N. Artemyev, M. Mai, and A. Surzhykov, *Phys. Rev. A* **86**, 052705 (2012).
 - [32] O. Novak, R. Kholodov, A. Surzhykov, A. N. Artemyev, and T. Stöhlker, *Phys. Rev. A* **97**, 032518 (2018).
 - [33] H. R. Reiss, *Prog. Quantum Electron.* **16**, 1 (1992).

- [34] A. Di Piazza, C. Müller, K. Z. Hatsagortsyan, and C. H. Keitel, *Rev. Mod. Phys.* **84**, 1177 (2012).
- [35] L. V. Keldysh, *Zh. Eksp. Teor. Fiz.* **47**, 1945 (1965) [*Sov. Phys. JETP* **20**, 1307 (1965)].
- [36] F. H. M. Faisal, *J. Phys. B* **6**, L89 (1973).
- [37] P. B. Corkum, *Phys. Rev. Lett.* **71**, 1994 (1993).
- [38] L. N. Gaier and C. H. Keitel, *Phys. Rev. A* **65**, 023406 (2002).
- [39] Y. I. Salamin, S. X. Hu, K. Z. Hatsagortsyan, and C. H. Keitel, *Phys. Rep.* **427**, 41 (2006).
- [40] D. B. Milošević, G. G. Paulus, D. Bauer, and W. Becker, *J. Phys. B* **39**, R203 (2006).
- [41] S. Selstø, E. Lindroth, and J. Bengtsson, *Phys. Rev. A* **79**, 043418 (2009).
- [42] M. S. Pindzola, S. A. Abdel-Naby, F. Robicheaux, and J. Colgan, *Phys. Rev. A* **85**, 032701 (2012).
- [43] M. Førre and A. S. Simonsen, *Phys. Rev. A* **90**, 053411 (2014).
- [44] T. Kjellsson, S. Selstø, and E. Lindroth, *Phys. Rev. A* **95**, 043403 (2017).
- [45] W. R. Johnson, S. A. Blundell, and J. Sapirstein, *Phys. Rev. A* **37**, 307 (1988).
- [46] V. M. Shabaev, I. I. Tupitsyn, V. A. Yerokhin, G. Plunien, and G. Soff, *Phys. Rev. Lett.* **93**, 130405 (2004).
- [47] T. J. Park and J. C. Light, *J. Chem. Phys.* **85**, 5870 (1986).
- [48] M. Drescher, M. Hentschel, R. Kienberger, M. Uiberacker, V. Yakovlev, A. Scrinzi, T. Westerwalbesloh, U. Kleineberg, U. Heinzmann, and F. Krausz, *Nature (London)* **419**, 803 (2002).
- [49] F. Krausz and M. Ivanov, *Rev. Mod. Phys.* **81**, 163 (2009).